Appendix- Fellows et al, 2020

TABLE OF CONTENTS

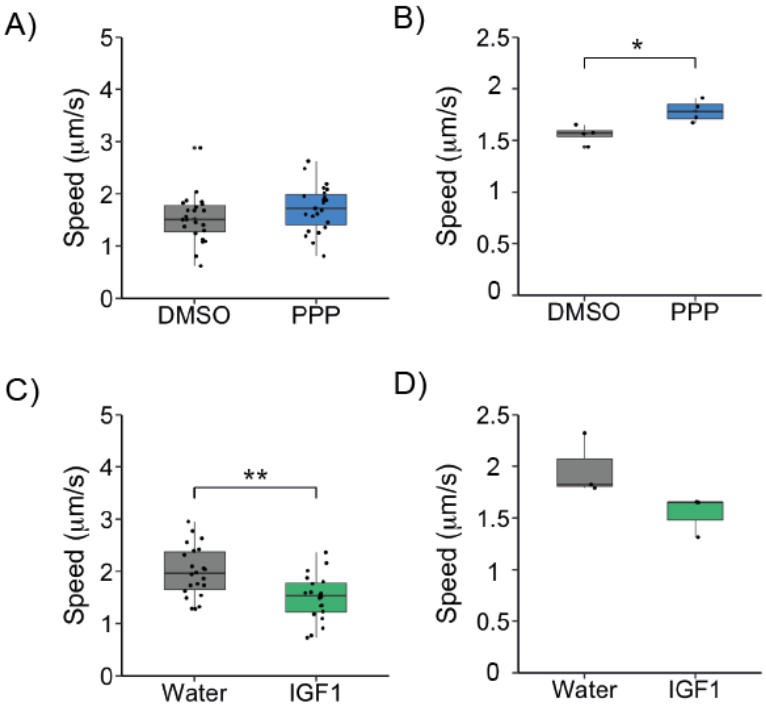

APPENDIX FIGURE S1- THE IGF1R PATHWAY INFLUENCES RETROGRADE AXONAL TRANSPORT OF SIGNALLING ENDOSOMES

A) Graph shows the average velocity of H_cT-containing organelles per axon after PPP treatment (P=0.15, Student's T-test, N=4 independent experiments, boxplot shows median, first and third quartiles. Upper/lower whiskers extend to 1.5 * the interquartile range, boxplot shows median, first and third quartiles).

B) Graph shows the average velocity of H_cT-containing organelles per experiment after PPP treatment (* P=0.017, Student's T-test, N=4 independent experiments, boxplot shows median, first and third quartiles. Upper/lower whiskers extend to 1.5 * the interquartile range).

C) Graph shows the average velocity of H_cT-containing organelles per axon after IGF1 treatment (** P=0.001, Student's T-test, N=3 independent experiments, boxplot shows median, first and third quartiles. Upper/lower whiskers extend to 1.5 * the interquartile range).

D) Graph shows the average velocity of H_cT-containing organelles per experiment after IGF1 treatment (P=0.09, Student's T-test, N=3 independent experiments, boxplot shows median, first and third quartiles. Upper/lower whiskers extend to 1.5 * the interquartile range).

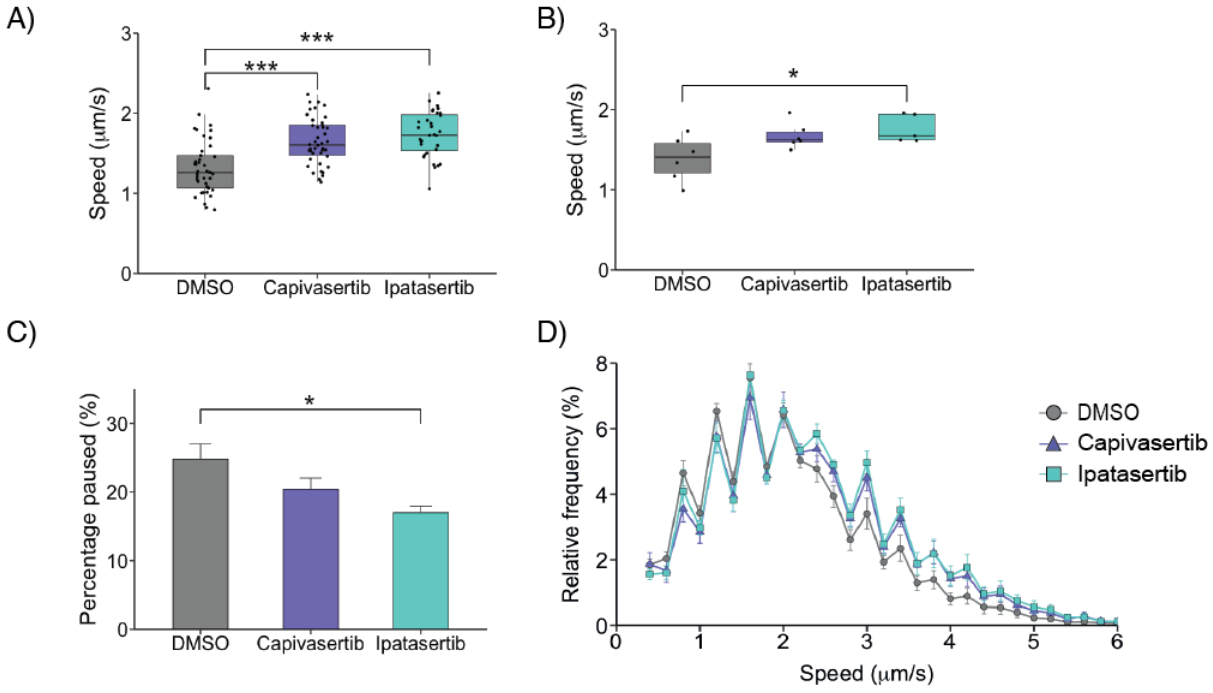

APPENDIX FIGURE S2- AKT INHIBITION INCREASES THE VELOCITY OF RETROGRADE SIGNALLING ENDOSOMES

A) Graph shows the average velocity of H_cT-containing organelles per axon after Capivasertib and Ipatasertib treatment for 45 mins before imaging (DMSO: 483 endosomes, 34 axons, 41,897 movements; Capivasertib: 658 endosomes, 43 axons, 49,841 movements; Ipatasertib: 605 endosomes, 32 axons, 41,485 movements, *** $P=2.44x10^{-7}$, One-way ANOVA, Tukey's post-hoc test: DMSO-Capivasertib *** $P=8.9x10^{-5}$, DMSO-Ipatasertib *** $P=2.5x10^{-5}$, N=6 independent experiments, boxplot shows median, first and third quartiles. Upper/lower whiskers extend to 1.5 * the interquartile range).

B) Graph shows the average velocity of H_cT-containing organelles per experiment after treatment with Capivasertib and Ipatasertib for 45 mins before imaging (* P=0.025, One-way ANOVA, Tukey's post-hoc test: DMSO-Capivasertib P=0.081, DMSO-Ipatasertib * P=0.028; N=6 independent experiments, boxplot shows median, first and third quartiles. Upper/lower whiskers extend to 1.5 * the interquartile range)

C) Graph shows the average pausing of H_cT-containing organelles per experiment after Capivasertib and Ipatasertib treatment for 45 mins before imaging (* P=0.027, One-way ANOVA, Tukey's post-hoc test: DMSO-Capivasertib P=0.20, DMSO-Ipatasertib * P=0.022, N=6 independent experiments, data shown are mean ± SEM).

D) Speed distribution profile of Capivasertib- and Ipatasertib-treated neurons and controls. Both compounds caused an increase in instantaneous velocities of H_cT-containing organelles compared to controls (N=6 independent experiments , data shown are mean $\pm$ SEM).

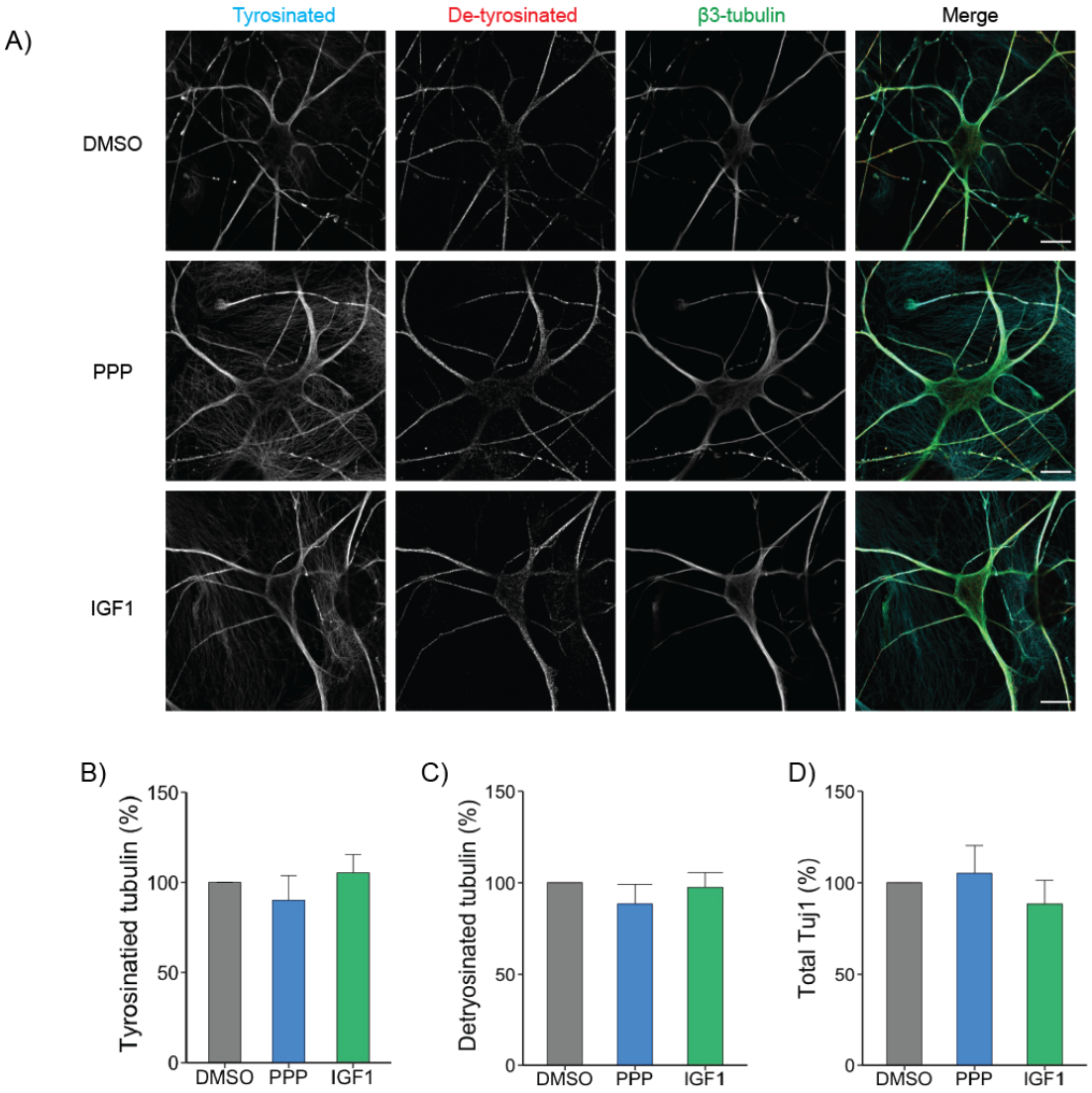

APPENDIX FIGURE S3- IGF1R MODULATION HAS NO EFFECT ON MICROTUBULE POST-TRANSLATIONAL MODIFICATIONS

A) Staining of tyrosinated and detyrosinated α-tubulin and β-tubulin in PMN after treatment with 1 μM PPP or 50 ng/ml IGF1 for 60 min. The scale bar is 10 μm.

B) Quantification of tyrosinated α-tubulin levels from A). Results were normalised relative to β-tubulin. IGF1R modulation had no effect on the amount of tyrosinated α-tubulin (DMSO- 100%, IGF1- 105.3 ± 9.9%, PPP- 89.9 ± 13.8%, P=0.55, one-way ANOVA, N= 4 independent experiments, 31-32 cells per condition, data shown are mean ± SEM).

C) Quantification of detyrosinated α-tubulin levels from A). Results were normalised relative to β-tubulin. There was no change after treatment (DMSO- 100%, PPP-88.2 $\pm$ 10.9%, IGF1- 97.5 $\pm$ 8.0%, P=0.55, one-way ANOVA, N=4 independent experiments, 31-32 cells per condition, data shown are mean $\pm$ SEM).

D) Quantification of β-tubulin levels from A). Treatment with PPP or IGF1 did not affect the amount of β-tubulin present in PMN (DMSO-100%, PPP- 105 $\pm$ 15.2%, IGF1- 87.9 $\pm$ 13.1%, P=0.59, one-way ANOVA, N=4 independent experiments, 31-32 cells per condition). Data shown are mean $\pm$ SEM.

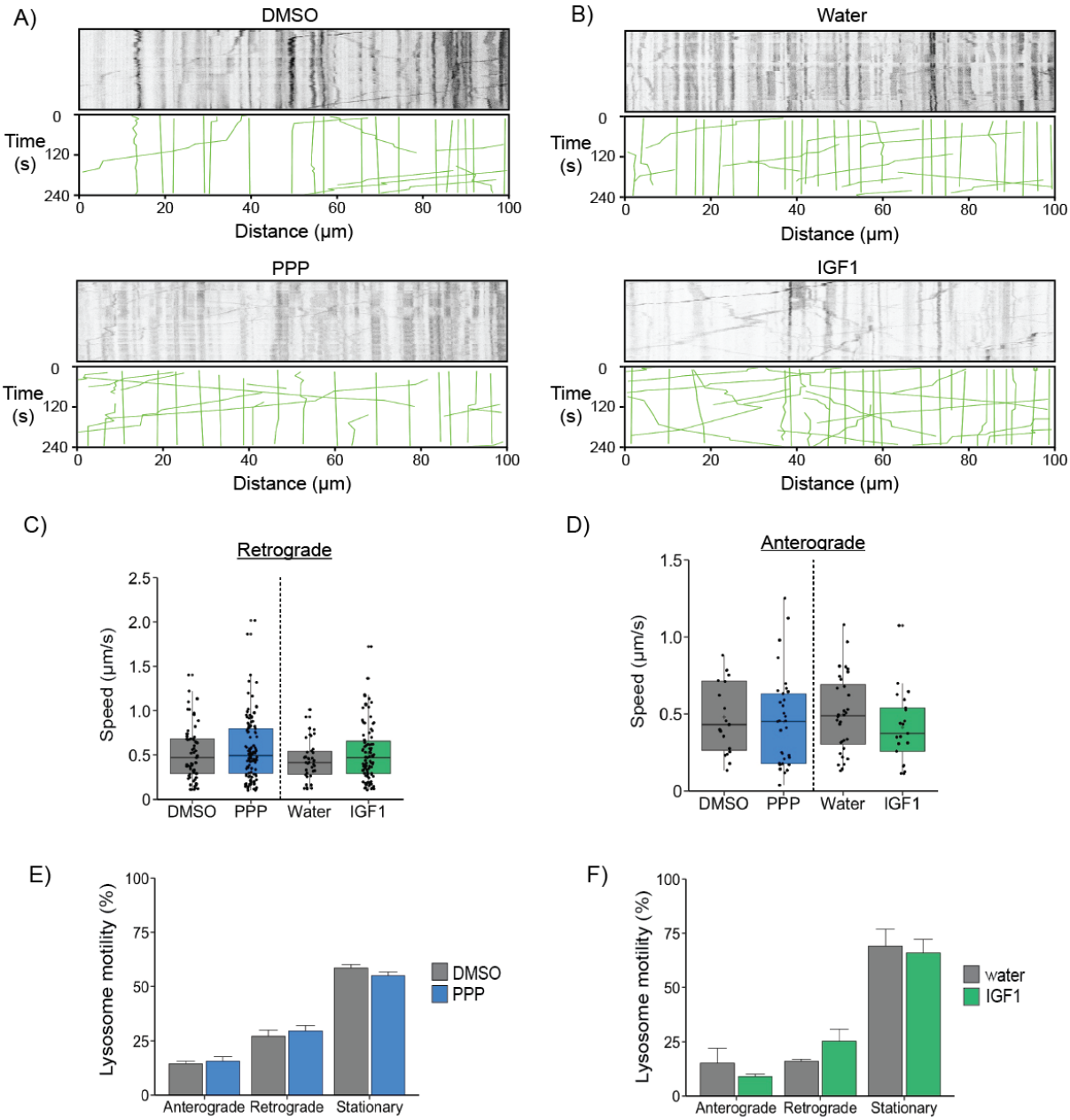

APPENDIX FIGURE S4- IGF1R ACTIVITY DOES NOT AFFECT AXONAL TRANSPORT OF LYSOSOMES

A) Kymographs of LysoTracker™ Green DND-26 labelled lysotracker in DIV 6 PMN after treatment with 1 µM PPP or control for 45 min.

B) Kymographs of LysoTracker™ Green DND-26 labelled lysotracker in DIV 6 PMN after treatment with 50 ng/ml IGF1 or control for 45 min.

C) Analysis of IGF1R modulation on retrograde lysosomal velocity. Neither PPP or IGF1 treatment had a significant effect on retrograde transport of lysosomes (DMSO: 0.53 ± 0.04 μm/s, cargo- 65, N=2 independent experiments; PPP: 0.57 ± 0.03 μm/s, cargo- 112, N=3 independent experiments; P= 0.41, Student's T-test; water: 0.44 ± 0.04 μm/s, cargo- 38, N=3 independent experiments; IGF1: 0.52 ± 0.03 μm/s, cargo- 91, N=3 independent experiments, P= 0.13, Student's T-test, boxplot shows median, first and third quartiles. Upper/lower whiskers extend to 1.5 * the interquartile range).

D) Analysis of IGF1R modulation on anterograde lysosomal velocity. PPP and IGF1 caused no significant change in anterograde transport rates (DMSO: 0.48 ± 0.05 μm/s, cargo- 19, videos- 13, N= 2 independent experiments; PPP: 0.4 ± 0.05 μm/s, cargo- 33, videos- 22, N= 3 independent experiments; P= 0.68, Student's T-test; water: 0.49 ± 0.04 μm/s, cargo- 32, N=3 independent experiments video- 13; IGF1: 0.41 ± 0.05 μm/s, cargo- 21, N=3 independent experiments, videos-21; P= 0.22, Student's T-test, boxplot shows median, first and third quartiles. Upper/lower whiskers extend to 1.5 * the interquartile range).

E) Analysis of the directionality of lysosome transport. There was no change in the directionality of lysosome transport after PPP treatment compared to controls (anterograde: DMSO- 14.4 ± 1.2%, cargo- 48; PPP- 15.6 ± 2.1%, cargo- 81, P= 0.65; retrograde: DMSO-27 ± 2.8%, cargo-88, PPP- 29.4 ± 2.5%, cargo- 160, P= 0.58; stationary: DMSO-58.6 ± 1.6%, cargo- 194; PPP- 55 ± 1.8%, cargo- 295, P= 0.24, Student's T-test, N=2 for DMSO and N=3 for all other conditions, data shown are mean ± SEM).

F) Analysis of the directionality of lysosome transport. IGF1 didn't change the directionality of lysosomes after treatment. Quantified from B) (anterograde: water- 15.1 ± 6.9%, cargo- 55; IGF- 8.9 ± 1.1%, cargo- 39, P= 0.53; retrograde: water- 15.9 ± 1.0%, cargo- 55, IGF-25.3 ± 5.4%, cargo- 120, P= 0.22; stationary: water- 69 ± 7.9%, cargo- 232, IGF- 65.8 ± 6.3 %, cargo-290, P= 0.783, Student's T-test, N=2 for DMSO and N=3 for all other conditions, data shown are mean ± SEM).

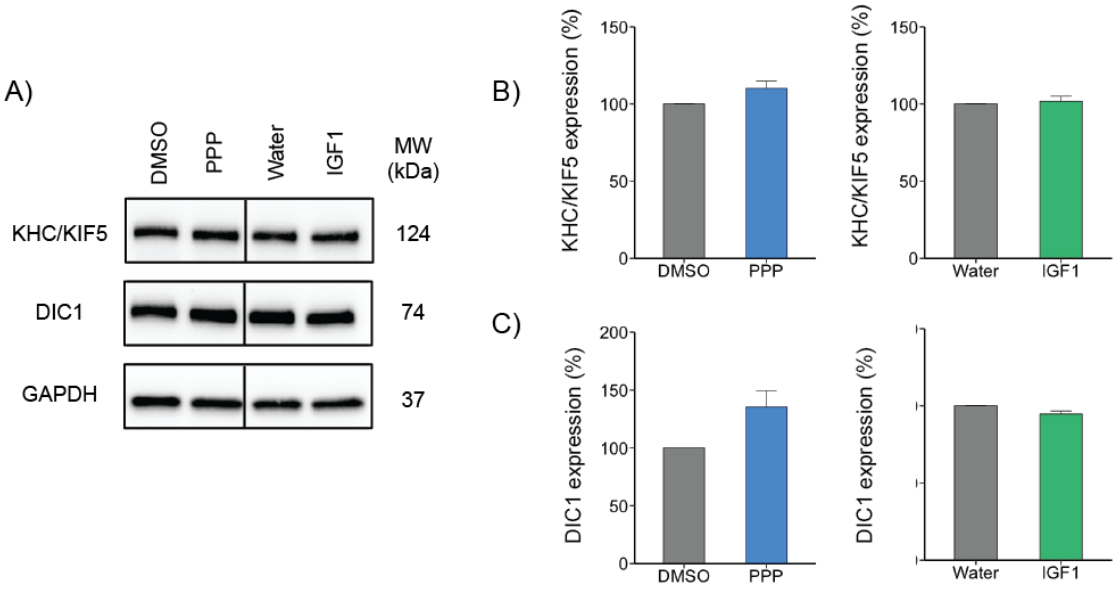

APPENDIX FIGURE S5- IGF1R MODULATION HAS NO EFFECT ON THE EXPRESSION OF CYTOPLASMIC DYNEIN OR KINESIN-1

A) PMN were treated with 1 μM PPP or 50 ng/ml IGF1 for 60 min and the expression of dynein intermediate chain (DIC1) and kinesin-1 (KHC/KIF5) were assessed via western blot. All proteins were assessed on the same blot along with proteins in Fig5.

B and C) Quantification of western blots in A). Protein levels were normalised to GAPDH. There was no significant change in levels of both motor proteins after treatment with PPP (KHC/KIF5: DMSO-100%, PPP-110.2 ± 4.7%, N=3 independent experiments, P=0.16; DIC1: DMSO-100%, PPP-135 ± 14.1%, N=5 independent experiments, P=0.067, Student's T-test) or IGF1 (KHC: water-100%, IGF1-101.76 ± 3.2%, N=3, P=0.63; DIC: water-100%, IGF1-94.7 ± 2.1%, N=3 independent experiments, P=0.12, Student's T-test, data shown are mean ± SEM).

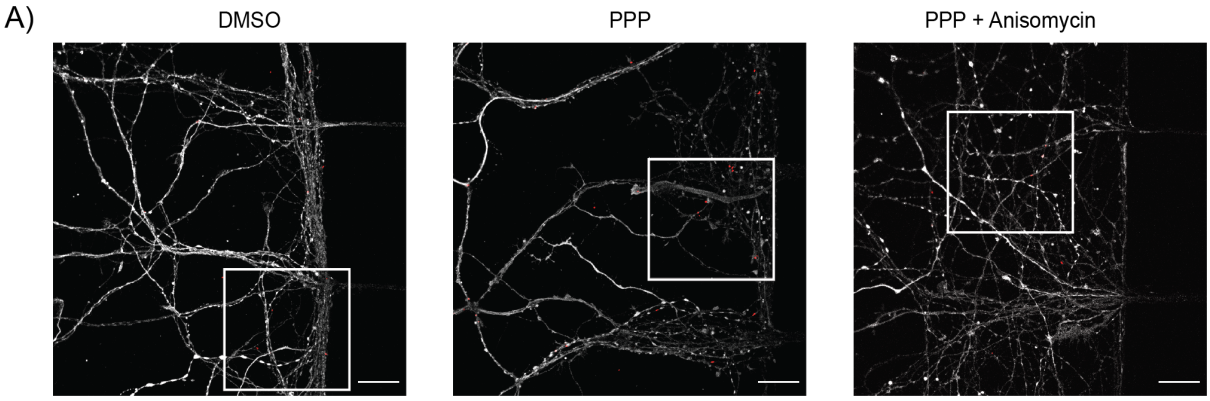

APPENDIX FIGURE S6- EXAMPLE IMAGES FROM PUROMYCIN-PLA

A) Puromycin-PLA images from the axonal compartment of PMN treated with PPP grown in microfluidic devices. White box indicates the zoomed region shown in Fig 6. Scale bars are 25 μm. White- β3-tubulin.

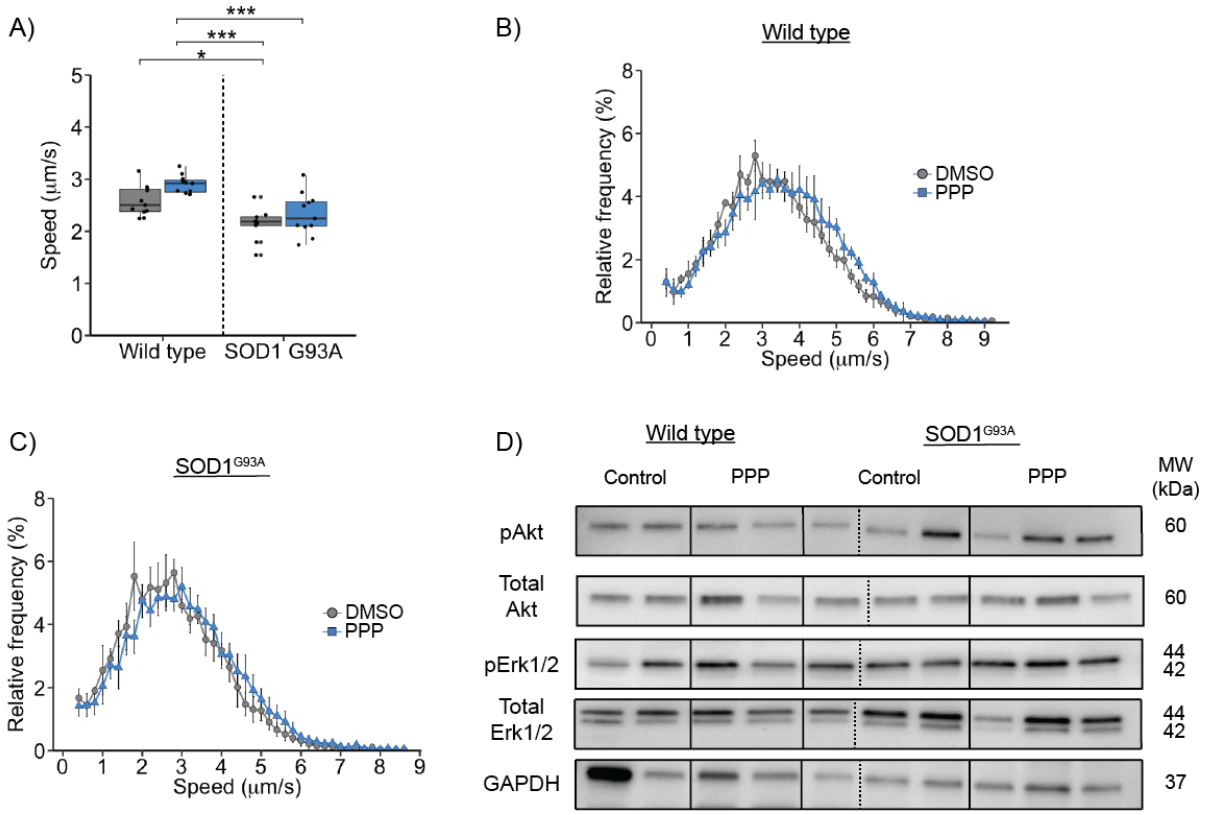

APPENDIX FIGURE S7- IGF1R INHIBITION INCREASES THE RATE OF RETROGRADE AXONAL TRANSPORT IN AN ALS MOUSE MODEL

A) The graph shows the average velocity of H_cT-containing organelles per video (P=0.019 (treatment), P= $3.83x10^{-6}$ (genotype), two-way ANOVA, Tukey's post-hoc text, WT-control: $SOD1^{G93A}$- control, * P=0.01 ;WT-control: WT-PPP, P=0.09; WT-PPP: $SOD1^{G93A}$- control, *** P=0.00001; WT-PPP: $SOD1^{G93A}$-PPP, *** P=0.0005, N=4 independent experiments for all conditions).

B) and C) Speed distribution graphs of wild type and $SOD1^{G93A}$ mice treated with PPP (blue squares) or vehicle control (grey circles). Graphs show increase in instantaneous velocities in both wild type and $SOD1^{G93A}$ mice. N=4 independent experiments. Data shown are mean ± SEM.

D) Example western blot of sciatic nerve lysates from wild type and $SOD1^{G93A}$ mice treated with either PPP or vehicle control were probed for pAKT (Ser473), total Akt, pErk1/2 (Thr 202/ Tyr 204) and total Erk1/2. Dashed line indicated where blots have been joined.